scientific reports

Check for updates

OPEN

Knockout or inhibition of DHPS suppresses ovarian tumor growth and metastasis by attenuating the TGFβ pathway

Guannan Zhao[1,2], Xinxin Zhao[3], Ziping Liu[3], Baojin Wang[3], Peixin Dong[4], Hidemichi Watari[4], Lawrence M. Pfeffer[1,2], Gabor Tigyi[5], Wenjing Zhang[6]✉ & Junming Yue[1,2]✉

Deoxyhypusine synthase (DHPS) is an enzyme encoded by the DHPS gene, with high expression in various cancers, including ovarian cancer (OC). DHPS regulates the translation initiation factor EIF5A, and EIF5A2 knockout inhibits OC tumor growth and metastasis by blocking the epithelial-to-mesenchymal transition (EMT) and the TGFβ pathway. In this study, we show that DHPS is amplified in OC patients, and its elevated expression correlates with poor survival. Using lentiviral CRISPR/Cas9 vectors for DHPS knockout, we observed EMT inhibition in SKOV3 and OVCAR8 cells through suppressed hypusination and reduced EIF5A2 expression. Inhibition of DHPS activity with GC7 similarly blocked hypusination and EMT. Disrupting DHPS expression, either genetically or pharmacologically, inhibited primary tumor growth and metastasis in OC mouse models. These findings suggest that targeting DHPS and inhibiting hypusination could be promising strategies for OC treatment.

Keywords DHPS, EIF5A, Ovarian cancer, EMT, Metastasis, TGFβ, Hypusination, GC7, Orthotopic OC mouse models

Abbreviations

OC	ovarian cancer
DHPS	deoxyhypusine synthase
EIF5A	eukaryotic translation initiation factor 5 A
EMT	epithelial-to-mesenchymal transition
KO	knockout
GC7	N1-guanyl-1,7-diaminoheptane
HGSC	high-grade serous carcinoma

Ovarian cancer (OC) is a highly lethal gynecological malignancy, presenting significant challenges for effective treatment and patient survival[1]. Despite recent advancements in treatment strategies, the five-year survival rate for OC remains low. Most deaths occur in patients with high-grade serous OC with widespread metastasis within the peritoneal cavity (advanced stage)[2]. Detecting ovarian cancer at an early stage is difficult because it is more likely to spread through intraperitoneal dissemination rather than via blood vessels or lymphatics[3]. Current diagnosis by using the combination of CA125 and HE4 as biomarkers, which have limited sensitivity and specificity in the early stages of the disease[4].

Epithelial-mesenchymal transition (EMT) is a complex phenotypic switch characterized by the loss of adherence junctions and the acquisition of a mesenchymal phenotype, which promotes motility and invasion. Emerging evidence suggests that EMT plays a critical role in tumor initiation, progression, invasion, and

[1]Department of Pathology and Laboratory Medicine, Collage of Medicine, the University of Tennessee Health Science Center, Memphis, TN 38163, United States. [2]Center for Cancer Research, Collage of Medicine, the University of Tennessee Health Science Center, Memphis, TN 38163, USA. [3]Department of Obstetrics and Gynecology, The Third Hospital of Zhengzhou University, Zhengzhou 450003, Henan, China. [4]Department of Obstetrics and Gynecology, Hokkaido University School of Medicine, Hokkaido University, Sapporo 060-8638, Japan. [5]Department of Physiology, Collage of Medicine, the University of Tennessee Health Science Center, Memphis, TN 38163, USA. [6]Department of Genetics, Genomics & Informatics, Collage of Medicine, University of Tennessee Health Science Center, Memphis, TN 38163, USA. ✉email: wzhang67@uthsc.edu; jyue@uthsc.edu

metastasis[5–7]. The role of EMT in ovarian cancer chemoresistance and metastasis has been extensively investigated[8–10].

Eukaryotic initiation factor 5 A (EIF5A) is the only known protein containing the hypusine residue[11]. EIF5A1 and EIF5A2 are isoforms of EIF5A, which share 84% sequence identity and 94% similarity[12]. EIF5A1 exhibits ubiquitous expression across human tissues, whereas EIF5A2 is expressed in brain and testis[13]. Located in chromosome 3q26, EIF5A2 was initially identified in OC and demonstrated significantly higher expression levels in OC compared to normal ovaries[14]. EIF5A2 is associated with a more aggressive and advanced disease state and significantly associated with patient poor survival[15–17]. Our recent findings have elucidated that EIF5A2 induces EMT by activating the TGFβ pathway in OC cells and knockout (KO) of EIF5A2 effectively inhibits OC progression[18]. Deoxyhypusine synthase (DHPS) is an enzyme encoded by the *DHPS* gene that contributes to the maturation of EIF5A. It cleaves polyamine spermidine and helps to transfer the 4-aminobutyl group to the lysine 50 residue of the EIF5A precursor. Subsequently, the pre-mature EIF5A is hydroxylated by deoxyhypusine hydroxylase (DOHH)[19,20]and leading to the formation of mature EIF5A. Accumulating evidence suggests that DHPS is highly expressed in multiple cancers, including OC, and contributes to tumor development and progression. DHPS expression is associated with poor patient survival in breast cancer and glioma[21,22]. Nevertheless, the role of DHPS in OC progression and metastasis remains unexplored. Inhibition of the DHPS using its inhibitor GC7, selectively inhibits the production of biologically active forms of EIF5A protein[23]. GC7 has been shown to effectively inhibit hypusination, EMT and block the EIF5A2 activity in various cancers[22,24–26], indicating its therapeutic potential in inhibiting cancer progression and metastasis.

In the present study, we investigated the role of DHPS in OC progression and metastasis and evaluated the translational significance of targeting DHPS using its inhibitor GC7 in vitro in OC cells and in vivo in orthotopic OC mouse models. We observed that inhibiting DHPS expression through genetic or pharmacological approaches resulted in the inhibition of primary ovarian tumor growth and metastasis by suppressing EMT and suppressing the TGFβ pathway. Collectively, our study provides comprehensive insights into the role of DHPS in OC metastasis and highlights its potential as a therapeutic target using GC7 by inhibiting hypusination and EIF5A, which may offer a strategy for developing novel OC treatment approaches.

Results

DHPS is highly expressed, and its expression is correlated with OC patient poor survival

To assess the clinical relevance of DHPS expression, we analyzed data from ovarian cancer (OC) patients in the TCGA database. The *DHPS* gene was amplified in 10.1% (59/584 cases) and showed deep deletion in 0.34% (2/584 cases) in the Firehouse Legacy dataset (Fig. 1a). In the Nature, 2011 dataset, we observed amplification in 7.77% (38/489 cases) and deep deletion in 0.2% (1/489 cases). Additionally, the Pan Cancer Atlas dataset revealed 7.71% alterations, including 7.02% (48/584 cases) amplification, 0.17% deep deletion, and 0.34% mutations (2/584 cases). These genetic alterations in *DHPS* have a significant impact on patient survival. Moreover, based on the three datasets, the overall survival of OC patients was significantly shorter in 145 patients with *DHPS* gene alterations compared to the 1512 patients without alterations (Fig. 1b).

To examine the expression of DHPS at the mRNA level, we analyzed various cancer samples using the GENT2 database and compared them with normal samples[27]. We found that DHPS was upregulated in cancers of the prostate, skin, breast, ovarian, thyroid, and uterus. Specifically, 1516 OC cases were compared to 92 normal samples, and DHPS expression was significantly upregulated (Fig. 1c). Analysis of DHPS expression in OC patient samples from the Human Protein Atlas revealed that DHPS exhibited strong cytoplasmic staining compared to adjacent normal tissues (Fig. 1d). DHPS was expressed in the plasma and nuclear membrane in most OC patients. However, in some cases, DHPS expression was also observed in the cell nuclei. To independently validate these findings, we performed immunohistochemical staining of DHPS in sections of human high-grade serous carcinoma (HGSC) from three patients. In one case, we observed aberrant expression of DHPS in the cell nuclei (Fig. 1e). DHPS was expressed in both cellular plasma and cell nuclei in two cases (Fig. 1f).

Furthermore, we analyzed the correlation between DHPS expression and survival in 1656 OC patients from the Kaplan-Meier Plotter database[28]. We found that patients with high DHPS expression demonstrated significantly poorer overall survival compared to those with low DHPS expression (Fig. 1g). The association of DHPS with overall survival in patients with different stages or cancer types were also analyzed and shown in Fig. S1. The median overall survival for the high DHPS expression group was 41.97 months (about 3 and a half years), whereas the low DHPS expression group had a median overall survival of 45.77 months (about 4 years). Our results demonstrate that DHPS is highly expressed in OC and is significantly associated with poor overall survival in OC patients.

Lentiviral CRISPR/Cas9 nickase vector-mediated DHPS KO inhibits hypusination, EIF5A2 and EMT in OC cells

We previously reported that the SKOV3 and OVCAR8 cell lines exhibited high endogenous expression of EIF5A2[18]. Knockout of EIF5A2 in both cell lines resulted in the inhibition of EIF5A2 hypusination, and attenuation of the TGFβ pathway leading to EMT inhibition. Hypusination of EIF5A2 is essential for its maturation and is achieved through DHPS-mediated deoxyhypusine modification on EIF5A. To investigate the impact of DHPS-mediated EIF5A hypusination, we knocked out DHPS in SKOV3 and OVCAR8 cells. The KO of DHPS led to the inhibition of EIF5A hypusination and EIF5A expression, resulting in a reversal of the EMT phenotypic switch, as shown by upregulation of epithelial cell markers, cytokeratin-7, and E-cadherin, and downregulation of mesenchymal markers, β-catenin and Vimentin (Fig. 2a, b). To further characterize the EMT phenotype switch, we treated SKOV3 and OVCAR8 cells with 6 ng/ml of TGFβ for 24 h and imaged the cell morphology thereafter (Fig. 2c). TGFβ-treated control cells showed a fibroblast-like mesenchymal morphology, which was not evident in the DHPS KO cells.

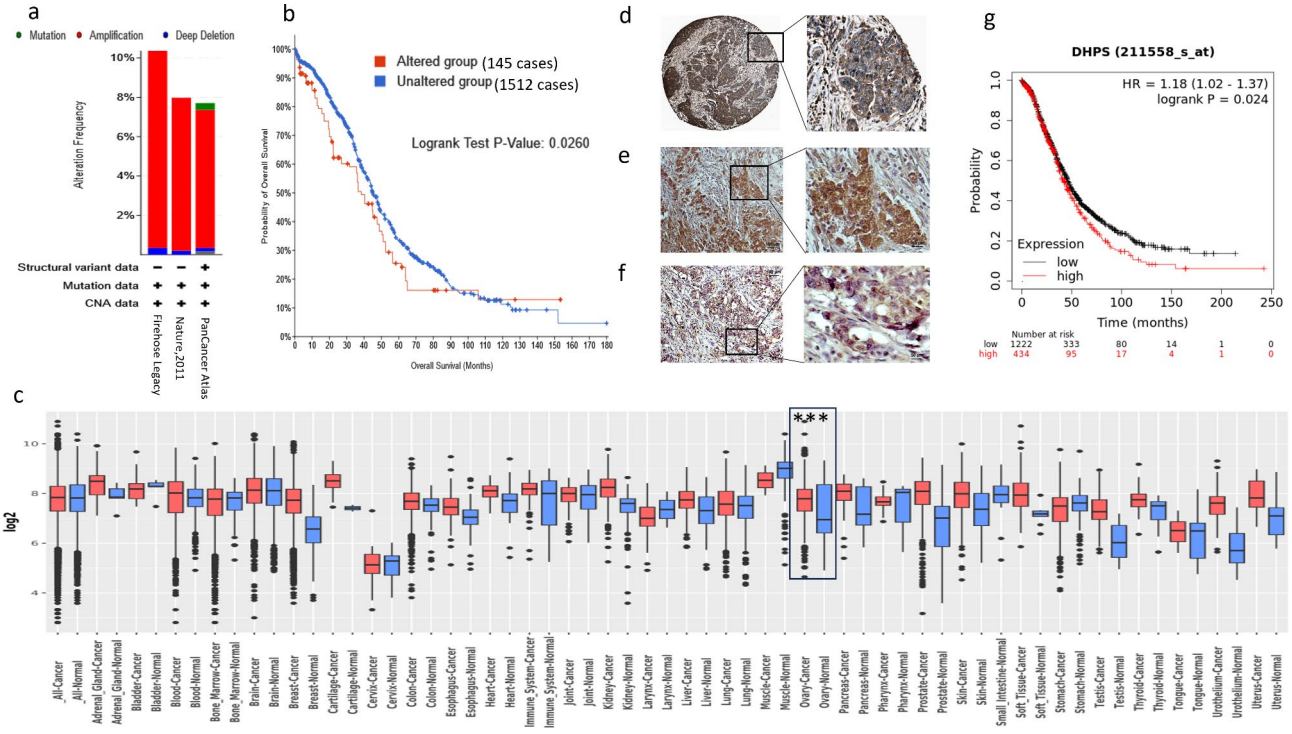

Fig. 1. *DHPS* Gene Expression and Correlation with Patient Survival (**a**) Genetic alterations of *DHPS* in OC patients were analyzed using three TCGA datasets: Firehose Legacy, Nature 2011, and PanCancer Atlas. (**b**) Correlation between *DHPS* Genetic Alterations and Patient Survival Overall survival analysis comparing the group with *DHPS* genetic alterations (145 cases) to the unaltered group (1512 cases) across all patients in the three different datasets. (**c**) DHPS expression levels were examined in different cancers, including OC patients, and compared to normal control samples. Significant differences were indicated with a black box (***$p < 0.001$). (**d**) Immunohistochemical staining of DHPS expression in OC sections from the Human Protein Atlas. e, f. DHPS expression in sections of HGSC was immunohistochemically stained in the cell nuclei (e) and in both the cytoplasm and the cell nuclei (**f**). g. The overall survival of OC patients was compared based on DHPS expression levels, revealing a significant association (*$p < 0.05$) between high DHPS expression and patient survival.

Inhibition of DHPS using GC7 led to suppression of hypusination, EIF5A2 expression and EMT in OC cells

To investigate the impact of DHPS inhibition on hypusination, we treated both SKOV3 and OVCAR8 cells with DHPS inhibitor GC7. GC7 treatment significantly suppressed hypusination in OC cells, indicating the effective inhibition of DHPS activity. We also assessed the effect of GC7 on EIF5A2 expression. Remarkably, GC7 treatment decreased EIF5A2 expression levels in both cells. In addition, we investigated the effect of GC7 on the EMT phenotype. GC7 treatment led to the inhibition of the EMT as shown by a significant upregulation of epithelial markers, including cytokeratin-7 and E-cadherin, and downregulation of mesenchymal markers, such as β-catenin and Vimentin (Fig. 3a, b). To assess the impact of DHPS inhibition on cell morphology, we examined the treated OC cells under the microscope. Control OC cells exhibited a typical mesenchymal morphology, characterized by a fibroblast-like appearance (Fig. 3c). GC7 treated cells showed less expression of DHPS, Vimentin, and increased Cytokarentin-7 (Fig. S2). In contrast, OC cells treated with GC7 displayed a more epithelial-like phenotype.

KO or inhibition of DHPS led to the inhibition of cell proliferation and survival in OC cells

To investigate the functional consequences of DHPS loss in OC cells, we evaluated cell survival and proliferation in SKOV3 and OVCAR8 cells. We performed cell colony formation assays to assess cell survival in DHPS KO and control cells. The results clearly demonstrated that the loss of DHPS expression significantly inhibited cell survival in both SKOV3 and OVCAR8 cells (Fig. 4a and b). To examine cell proliferation, we also conducted MTT assays. KO of DHPS reduced cell proliferation at all three time points (24, 48, and 72 h) in both SKOV3 and OVCAR8 cells (Fig. 4c and d). To further investigate the impact of DHPS inhibition, we treated SKOV3 and OVCAR8 cells with 20 μM of GC7 and evaluated cell survival using the colony formation assay. GC7 treatment significantly inhibited cell survival in both cell lines (Fig. 5a and b). Furthermore, we examined the effect of GC7 on cell proliferation by treating SKOV3 and OVCAR8 cells with three different doses of GC7 (0, 10, and 20 μM) at four time points (24, 48, 72, and 96 h). The results revealed significant inhibition of cell proliferation in both SKOV3 and OVCAR8 cells upon GC7 treatment (Fig. 5c and d).

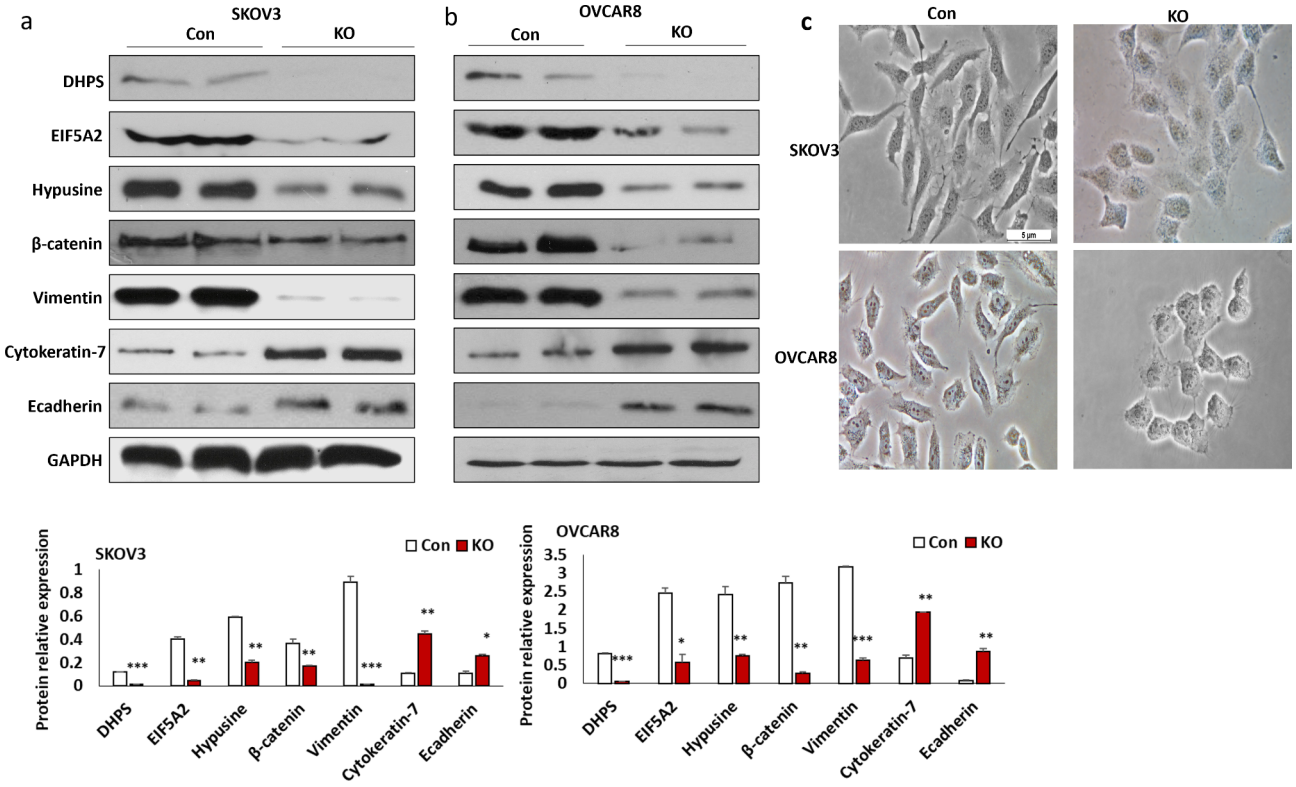

Fig. 2. KO of DHPS expression inhibits hypusination, EIF5A2 and EMT in OC cells. a, b. Western blot analysis showing the levels of DHPS, hypusine, EIF5A2, and EMT markers in DHPS knockout (KO) and control SKOV3 (**a**) and OVCAR8 (**b**) cells. The lower panel shows the quantification analysis. (*$P < 0.05$; **$P < 0.01$; ***$P < 0.001$) c. Morphological changes in DHPS KO and control SKOV3 and OVCAR8 cells treated with 6 ng/ml of TGFβ for 24 h, and their cell morphology was imaged under a microscope.

KO or inhibition of DHPS expression led to the inhibition of cell migration and invasion in OC cells

The loss of DHPS expression in OC cells was found to have a suppressive effect on EMT, suggesting that blocking EIF5A2 hypusination may also impact cell motility and invasion. To investigate the impact of DHPS expression on cell migration in OC cells, we performed cell migration assays using transwell plates. DHPS KO and control SKOV3 and OVCAR8 cells were seeded to migrate through the transwell membrane for 8 h. The results revealed that cell migration of DHPS KO cells was significantly inhibited compared to the control cells in both cell lines (Fig. 6a). Next, we examined the effect of DHPS expression on cell invasion in OC cells using Matrigel-coated transwell plates. Notably, KO of DHPS expression resulted in a substantial reduction in cell invasion in both SKOV3 and OVCAR8 cells compared to the control cells (Fig. 6b). To further investigate the impact of DHPS inhibitor GC7, we treated SKOV3 and OVCAR8 cells with 20 μM of GC7 and assessed cell migration and invasion using the transwell assays. Treatment with GC7 significantly reduced cell migration and invasion in both SKOV3 and OVCAR8 cell lines (Fig. 6c and d).

KO or inhibition of DHPS attenuated TGFβ signaling pathway in OC cells

We previously found that KO of EIF5A2 attenuates the TGFβ pathway in OC cells (18). To investigate whether KO or inhibition of DHPS also influences the TGFβ pathway in OC cells, we treated DHPS KO and control SKOV3 and OVCAR8 cells with 6 ng/ml of TGFβ for different time points and examined the levels of phospho- and total SMAD2 using western blot analysis. The results showed that KO of DHPS led to a notable attenuation of the TGFβ signaling pathway in DHPS KO cells compared to the control cells (Fig. 7a and b). Similarly, following treatment with 20 μM of GC7, we observed a significant reduction in phospho-SMAD2 levels in both SKOV3 and OVCAR8 cells (Fig. 7c and d). These findings suggest that DHPS plays a critical role in regulating the TGFβ signaling pathway in OC cells, indicating that DHPS is involved in the modulation of TGFβ-induced cellular responses in OC.

KO or inhibition of DHPS suppressed primary ovarian tumor growth and metastasis by inhibiting hypusination modification of EIF5A2 and EMT in an orthotopic OC mouse model

We previously showed that KO of EIF5A2 inhibits OC growth and metastasis by attenuating the EMT and TGFβ pathway[18]. We hypothesized that DHPS is responsible for EIF5A2 maturation through the hypusination pathway, thus KO of DHPS may show a similar functional consequence. To test this hypothesis, we intrabursally injected 5×10^5 DHPS KO and control OVCAR8 cells into two-month-old immunodeficient NSG female mice.

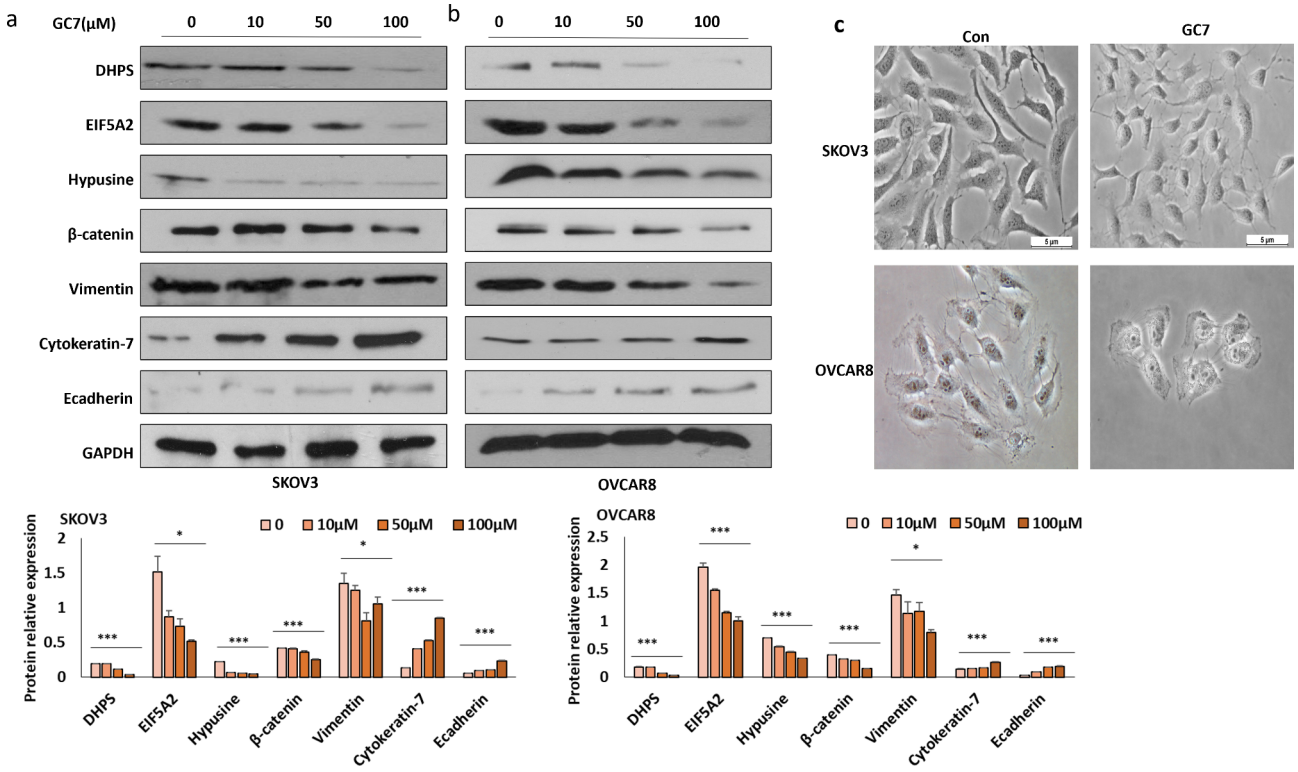

Fig. 3. GC7 inhibits hypusination, EIF5A2 and EMT in OC cells. a, b. Western blot analysis showing the levels of DHPS, hypusine, EIF5A2, and EMT markers in SKOV3 and OVCAR8 cells treated with different doses of GC7. The lower panel shows the quantification analysis. (*$P < 0.05$; **$P < 0.01$; ***$P < 0.001$) c. Morphological changes in SKOV3 and OVCAR8 Cells. SKOV3 and OVCAR8 cells were treated with 20 μM GC7 or vehicle for 24 h and then exposed to 6 ng/ml of TGFβ for an additional 24 h. Cell morphologies were imaged under a microscope.

Mice xenografted with DHPS KO exhibited marked inhibiting of primary OC and OC metastasis compared to the aggressive primary tumors and metastasis to multiple organs including omentum, liver, kidney, spleen, and intestine as observed in mice xenografted with control OVCAR8 cells. The primary ovarian tumor and metastasis in liver were shown in Fig. 8a and b. Histological analysis using H&E staining confirmed the absence of metastatic tumors in liver of mice injected with DHPS KO and control cells (Fig. 8c). To elucidate the molecular mechanisms underlying these observations, we examined DHPS, hypusine, EIF5A2, EMT markers, and pSMAD2 expression in primary ovarian tumors using western blotting. KO of DHPS resulted in the inhibition of hypusine and EIF5A2 expression, and downregulation of mesenchymal markers, including β-catenin and Vimentin, as well as p-SMAD2 expression while upregulation of epithelial markers such as cytokeratin-7 and E-cadherin were upregulated in DHPS KO cells (Fig. 8d). We also validated expression using immunostaining of tumor sections from the mouse ovaries with DHPS, Vimentin, Cytokeratin-7, and hypusine antibodies further corroborated these findings (Fig. S3).

To investigate whether GC7 suppresses ovarian tumor growth and metastasis by inhibiting DHPS, we evaluated the efficacy of GC7 in an orthotopic ovarian cancer mouse model. OVCAR8-Luc2 cells were intrabursally injected into NSG female mice and then treated with GC7 five days a week for four weeks. At five weeks following cell injection, tumors were dissected at necropsy for further analysis. Mice treated with GC7 had a significant reduction in primary ovarian tumor growth and metastasis compared to the vehicle-treated mice (Fig. 8e). Furthermore, found that tumors metastasized into multiple organs in vehicle-treated mice with metastasis in liver was shown by chemiluminescence, while mice treated with GC7 displayed lower metastasis (Fig. 8f), which was validated by H&E staining (Fig. 8g). To understand the underlying molecular mechanisms, we examined DHPS, EIF5A2, EMT markers, and pSMAD2 expression in primary ovarian tumors using western blotting. GC7 treatment inhibited EIF5A2 expression, and downregulated mesenchymal markers, including β-catenin and Vimentin, as well as p-SMAD2 expression. Conversely, epithelial markers such as cytokeratin-7 and E-cadherin were upregulated in GC7-treated tumors compared to vehicle group (Fig. 8h). Immunostaining of tumor sections from mouse ovaries with DHPS, Vimentin, Cytokeratin-7, hypusine, and Ki67 antibodies further supported these findings (Fig. S4 and S5). Our results indicate that the inhibition of DHPS by GC7 suppressed primary ovarian tumor growth and tumor metastasis by inhibiting EMT and attenuating the TGFβ pathway in orthotopic OC mouse models.

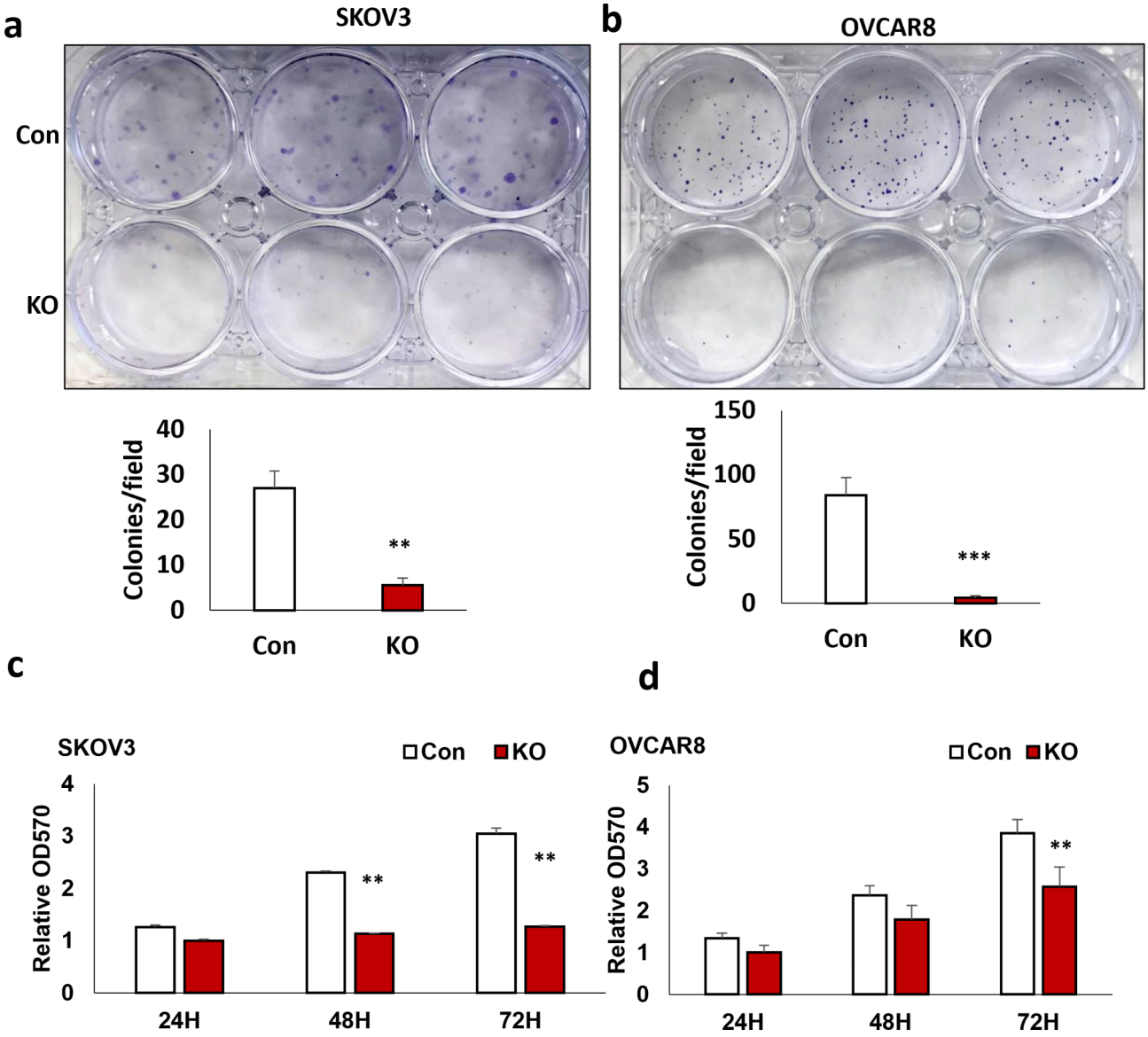

Fig. 4. KO of DHPS inhibits cell colony formation and proliferation in OC cells. **a**, **b**. Quantification of colony formation in DHPS KO and control SKOV3 and OVCAR8 cells (*$P < 0.05$; **$P < 0.01$). **c**, **d**. Cell proliferation analysis of DHPS KO and control SKOV3 and OVCAR8 cells using the MTT assay (*$P < 0.05$; **$P < 0.01$). Cell doubling time: SKOV3 control (37 h), SKOV3 DHPSKO (139 h), OVCAR8 control (24 h), OVCAR8 DHPSKO (35 h).

Discussion

The present study has offered valuable insights into the significance of DHPS in OC and its potential as a therapeutic target for OC treatment. Our findings demonstrate that DHPS is highly expressed in OC as well as in various other cancers, and its elevated expression is associated with poor patient survival in OC. Additionally, the DHPS gene is amplified in OC patients, further supporting its potential role in OC pathogenesis. KO of DHPS or inhibition of DHPS activity with GC7 effectively suppressed EMT by downregulating hypusination and EIF5A2 expression through attenuating the TGFβ pathway in OC cells. Both genetic and pharmacological approaches validate DHPS as a promising target for OC therapy.

Previous research has shown that DHPS is upregulated in breast cancer[21], lung cancer[29], and neuroblastoma[30], and its overexpression correlates with poor patient survival. Our study adds to the existing knowledge by revealing that DHPS is also upregulated or amplified in OC. Although DHPS deletion or mutation is rare and has not been thoroughly investigated for its impact on OC development, we found that DHPS amplification clearly correlates with poorer patient survival, making it a potential biomarker for early diagnosis and prognosis. Furthermore, the DHPS inhibitor GC7 suppressed EMT and tumor metastasis in various other cancer types, including hepatocarcinoma[25,31], oral cancer[24]and breast cancer[26]. Additionally, GC7 inhibits TGFβ-induced EIF5A hypusination and EMT, which is consistent with our findings described herein. In a previous report, we

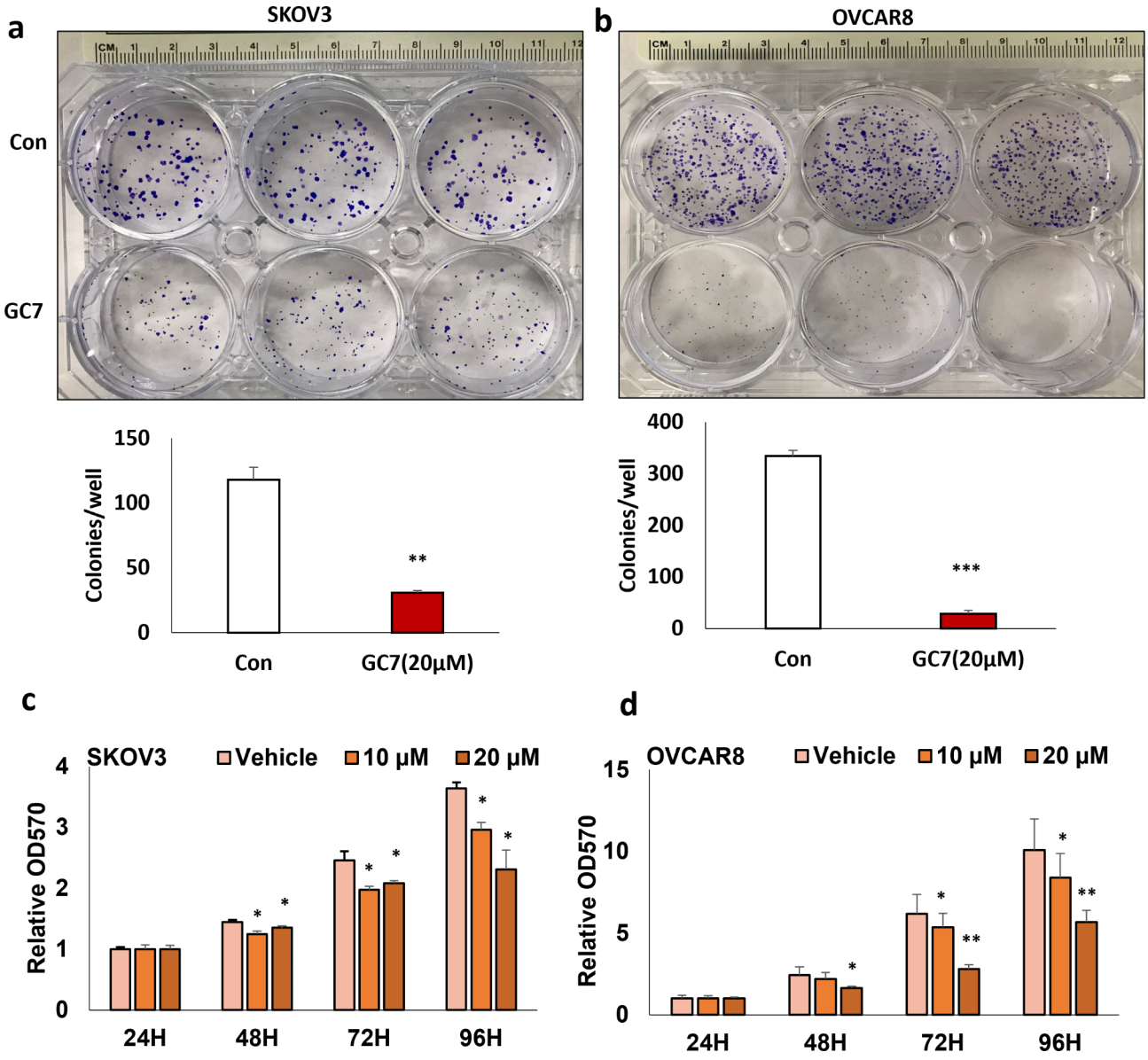

Fig. 5. GC7 inhibited cell colony formation and proliferation in OC cells. **a**, **b**. Quantification of colony formation in SKOV3 and OVCAR8 cells treated with 20 μM GC7 for two weeks (**$P < 0.01$; ***$P < 0.001$). c, d. Cell proliferation analysis in SKOV3 and OVCAR8 cells following treatment with 10 and 20 μM of GC7 for various time points, determined by the MTT assay (*$P < 0.05$; **$P < 0.01$; ***$P < 0.001$). Cell doubling time: SKOV3 vehicle (38 h), SKOV3 GC7 10 μM (46 h), SKOV3 GC7 20 μM (59 h), OVCAR8 vehicle (23 h), OVCAR8 GC7 10 μM (25 h), OVCAR8 GC7 20 μM (32 h).

demonstrated that TGFβ-induced EIF5A2 hypusination and EMT in OC, and KO of EIF5A2 suppressed OC growth and metastasis by inhibiting EMT and attenuating the TGFβ pathway[18]. Thus, the functional effects of genetic or pharmacological targeting of DHPS to block EIF5A2 maturation through hypusination is consistent with our studies on EIF5A2. DHPS may also function by activating multiple survival pathways, as it has been found to directly interact with ERK and be phosphorylated by ERK1/2 in HEK293 cells[29]. This suggests that the DHPS/EIF5A hypusination axis plays a critical role in tumor growth and metastasis by regulating various survival pathways, including TGFβ and ERK1/2, which both promote EMT in several cancers. Blocking DHPS activity using GC7 effectively reduces hypusinated EIF5A2 levels, which is critical for EMT and tumor invasion.

EMT is a key process that allows tumor cells to acquire migratory and invasive properties, and it is regulated by various signaling pathways, including TGFβ, Wnt, Notch and Hedgehog[32–36]. We previously demonstrated that TGFβ induces EMT in OC cells[37]. In this study, we uncovered a novel role of DHPS in mediating the TGFβ pathway to regulate EMT in OC, indicating that DHPS/EIF5A hypusination contributes to aggressive tumor metastasis in OC by promoting EMT through TGFβ pathway activation. Our in vivo experiments using orthotopic OC mouse models provided convincing evidence that disrupting DHPS expression through genetic or pharmacological means significantly inhibited primary ovarian tumor growth and metastasis. Moreover,

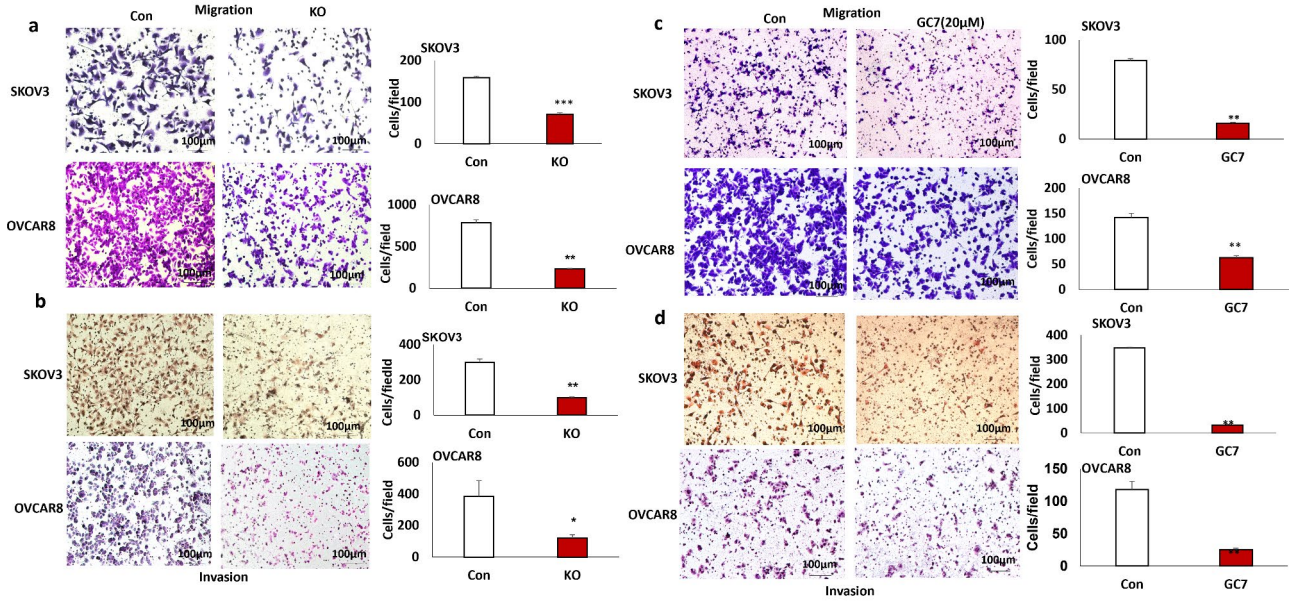

Fig. 6. KO or inhibition of DHPS inhibits cell migration and invasion in OC cells. (a) Cell migration analysis in DHPS KO and control SKOV3 or OVCAR8 cells using transwell plates. Migrated cells were stained with crystal blue and counted (**$P < 0.01$; ***$P < 0.001$). (b) Cell invasion analysis in both DHPS KO and control SKOV3 or OVCAR8 cells using Matrigel-coated plates. Invaded cells were stained with H&E and counted (*$P < 0.05$; **$P < 0.01$). (c) Cell migration analysis in SKOV3 or OVCAR8 cells treated with 20 μM GC7 using transwell plates. Migrated cells were stained with crystal blue and counted (**$P < 0.01$). (d) Cell invasion analysis in SKOV3 or OVCAR8 cells treated with 20 μM GC7 for 24 h, determined using Matrigel-coated plates. Invaded cells were stained with H&E and counted (**$P < 0.01$).

we confirmed that KO of DHPS or inhibition of DHPS using GC7 suppressed EMT and attenuated the TGFβ pathway in an in vivo mouse model. These findings strongly support the therapeutic potential of targeting DHPS in OC treatment by inhibiting DHPS/EIF5A-mediated hypusination.

Despite these promising findings, further investigations are warranted to fully understand the molecular mechanisms underlying DHPS-mediated effects on OC progression and metastasis. While we showed that KO or inhibition of DHPS attenuates the TGFβ pathway, the precise mechanism by which DHPS regulates TGFβ signaling remains unclear. Further studies are needed to elucidate how hypusination affects the stability, trafficking, or interaction of TGFβ receptors with other proteins.

Our study demonstrates that DHPS plays an important role in OC and has potential as a therapeutic target. By elucidating that DHPS regulates EMT, tumor growth, and metastasis, we pave the way for future research and the development of DHPS-targeted therapies for improved management of OC patients. The inhibition of DHPS activity presents a promising avenue for disrupting EMT and inhibiting tumor progression in OC, thereby offering new hope for more effective treatment strategies in the fight against this devastating disease.

Methods

Cell culture

The SKOV3 OC cell line was purchased from ATCC. It was cultured in DMEM (Dulbecco's Modified Eagle Medium) containing 10% fetal bovine serum (FBS) from Hyclone (Logan, UT), and 100 U/ml penicillin/streptomycin (PS) from Invitrogen (Carlsbad, CA). The OVCAR8 cell line was obtained from the National Cancer Institute and was cultured in RPMI 1640 medium with 10% FBS and 1% PS. Both OC cell lines were maintained in an incubator which was set at 37 °C in a humidified atmosphere containing 5% CO_2. No mycoplasma contamination was confirmed by luciferase assay from Lonza (Allendale, NJ).

Production of lentiviral vector

The lentiviral CRISPR/Cas9 nickase-mediated DHPS gene editing vectors were constructed by annealing two pairs of gRNA oligonucleotides and subcloning them into the BsmII site of the Lentiguide-puro vector (#52963, Addgene). The gRNAs were driven by the human U6 promoter. Two gRNA sequences, 5'AGGAAGTAGGGA ACGTGCTT and 5'GAACGCCTCTGCGCGCGCAG, were designed to target exon I of the DHPS gene. To generate DHPS KO stable cell lines, the lentiviral CRISPR/Cas9 nickase vectors were transduced into the SKOV3 and OVCAR8 ovarian cancer cells. The transduced cells were then selected using 2 μg/ml puromycin or 10 μg/ml blasticidin. As a control vector without gRNAs, LentiCas9-blast was used.

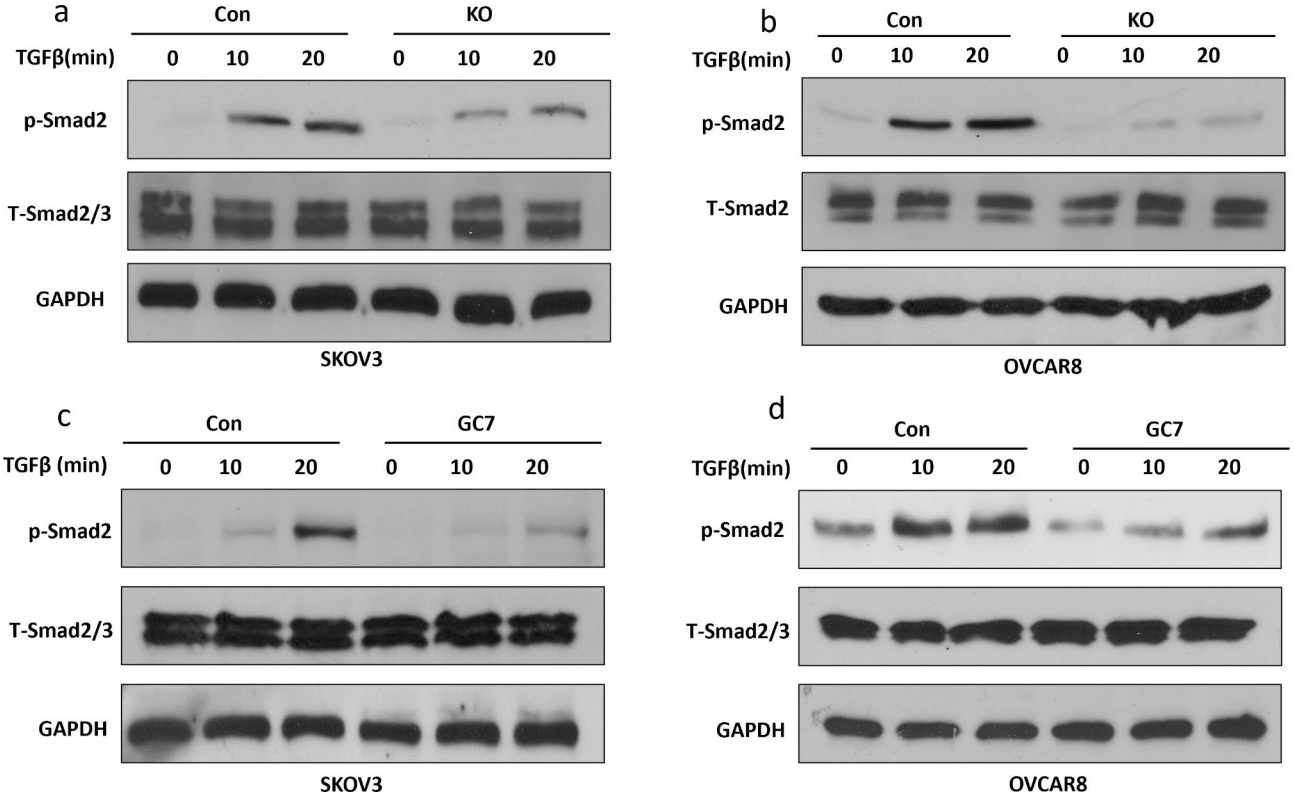

Fig. 7. KO or inhibition of DHPS attenuated the TGFβ signaling pathway in OC cells. **a**, **b**. Western blot analysis showing the expression of phospho- and total SMAD2 in DHPS knockout (KO) and control SKOV3 and OVCAR8 cells following treatment with 6 ng/ml TGFβ at the indicated time points. **c**, **d**. Western blot analysis showing the expression of phospho- and total SMAD2 in SKOV3 and OVCAR8 cells following treatment with 20 μM GC7 for 12 h and subsequent treatment with 6 ng/ml TGFβ at the indicated time points.

MTT assay

SKOV3 and OVCAR8 cells were transduced with lentiviral CRISPR/Cas9 nickase DHPS editing vectors, along with control or wild-type cells. 3000 cells per well were plated into 96-well plates and cultured for different time points (24, 48, and 72 h). Afterward, 10 μl of MTT reagent was added to each well and incubated for approximately 4 h. The reaction was terminated by adding 100 μl of detergent reagent and incubating at 22 °C in the dark for 2 h. Cell proliferation was assessed by measuring the absorbance at a wavelength of 570 nm.

Cell clonogenic survival assay

For the cell clonogenic survival assay, DHPS KO and control SKOV3 and OVCAR8 cells, or wild-type cells treated with GC7, were seeded onto 6-well plates and cultured for 2 weeks. The cells were then fixed with 70% ethanol and stained with crystal blue. Colonies were counted in triplicate for statistical analysis.

Cell migration assay

The cell migration assay was performed using transwell chambers (BD Falcon™, San Jose, CA) inserted into 24-well cell culture plates. SKOV3 and OVCAR8 cells (5×10^4) in 300 μl of serum-free culture medium were added to the upper chamber. In the lower chamber, culture medium containing 10% FBS was used as a chemoattractant. The cells were then cultured for 8 h. After incubation, the medium and non-migrated cells in the upper chamber were carefully removed. The migrated cells on the lower side of the membranes were fixed with methanol and stained with crystal violet. Images of the migrated cells were captured at 10X magnification, and cells from at least three different fields were counted for analysis.

Cell invasion assay

SKOV3 and OVCAR8 cells (3×10^5) were seeded in 300 μl of serum-free culture medium onto transwell plates that were pre-coated with Matrigel (BD BioSciences, San Jose, CA). In the bottom chamber of the invasion system, medium containing 10% FBS was added as a chemoattractant. After incubation overnight, the transwell inserts were fixed with methanol for 20 min. Then, they were stained with hematoxylin and eosin for 10 min. Images of the invaded cells were captured at 10X magnification. The invaded cells were counted in at least three different fields for further analysis.

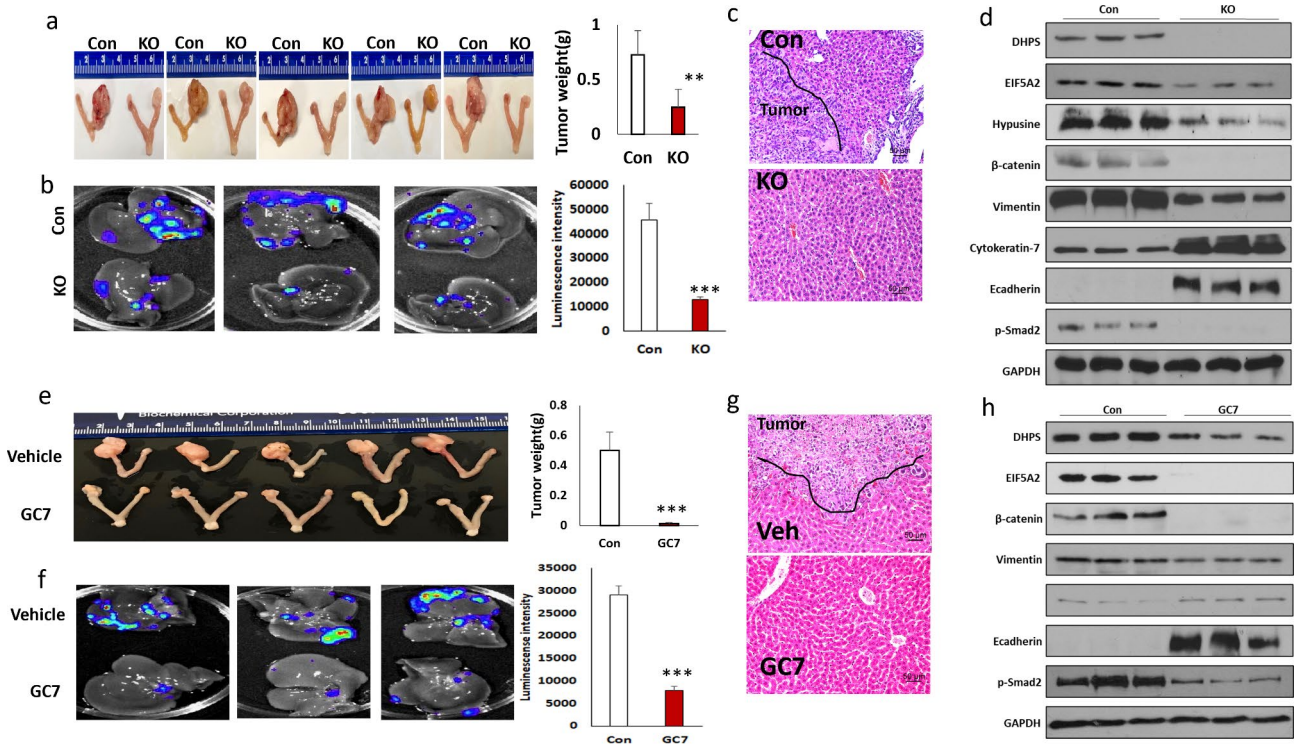

Fig. 8. KO or inhibition of DHPS using lentiviral CRISPR/Cas9 nickase vector suppressed primary ovarian tumor growth and metastasis in orthotopic OC mouse model. (**a**) Primary ovarian tumors dissected one month after intrabursal injection of DHPS KO and control OVCAR8 cells. Tumor weight in DHPS KO is significantly lower than in the control group ($n=5$, $^{**}P<0.01$). (**b**) Bioluminescence imaging of metastatic tumors in the liver of mice xenografted with DHPS KO and control cells ($n=3$, $^{**}P<0.01$). (**c**) Histopathological characterization of metastatic tumors from the liver of mice xenografted with DHPS KO and control cells using H&E staining. (**d**) Western blot analysis of DHPS, Hypusine, EIF5A2, p-SMAD2, and EMT markers in primary tumors of mice xenografted with DHPS KO and control cells. (**e**) Significant reduction in primary ovarian tumor weight in mice treated with GC7 compared to control ($^{***}P<0.001$). (**f**) Bioluminescence imaging of metastatic tumors in the liver of mice xenografted with GC7 treatment and the control group ($^{***}P<0.001$). (**g**) Histopathological characterization of metastatic tumors from the liver of mice xenografted with GC7 treatment and the control group using H&E staining. (**h**) Western blot analysis of DHPS, EIF5A2, p-SMAD2, and EMT markers in primary tumors of mice treated with GC7 and the control group ($^{**}P<0.01$; $^{***}P<0.001$).

Immunostaining

The paraffin-embedded (FFPE) blocks of fully de-identified ovarian serous carcinoma samples were obtained from the Tissue Services Core at the University of Tennessee Health Science Center (UTHSC). Hematoxylin and eosin (H&E) staining was performed by the Histology Core at UTHSC. For immunofluorescent staining, the slides were incubated overnight with primary antibodies against DHPS (1:200 dilution, Novus Biologicals, Centennial, CO), Hypusine (1:200 dilution, Millipore Sigma, Temecula, CA), Cytokeratin-7 (1:200 dilution, Abcam, Cambridge, UK), and Vimentin (1:200 dilution, Cell Signaling, Danvers, MA). After three rinses with PBST for 5 min each, Alexa 488- or 594-conjugated goat anti-rabbit or anti-mouse secondary antibodies (Invitrogen, Carlsbad, CA) were added and incubated for 1 h at room temperature. Cell nuclei were counterstained with DAPI (Vector Laboratories, Inc.; Burlingame, CA). Imaging was performed using a Zeiss LSM700 laser scanning confocal microscope to capture the images. For immunohistochemistry staining, the slides were incubated with antibody against DHPS (1:200 dilution, Novus Biologicals, Centennial, CO) overnight at 4°C. After three washes with PBST, the slides were then incubated with prediluted biotinylated horse anti-mouse/rabbit IgG (H + L) (Vector) at room temperature for 1 h. For visualization of reaction products, sections were treated with 3, 3¢-diaminobenzidine (DAB Substrate Kit; Vector), and then counterstained with Hematoxylin 7211 (Richard-Allan Scientific, Kalamazoo, MI).

Western blot

OC cells were collected using RIPA buffer (Thermo Scientific; Rockford, IL) supplemented with 1% Halt Proteinase Inhibitor Cocktail (Thermo Scientific; Rockford, IL). An equal amount of protein (100 µg/lane) was loaded onto 10% SDS-PAGE gels and transferred onto nitrocellulose membranes. The membranes were then blocked with 5% nonfat milk for 1 h and incubated with primary antibodies against the following proteins:

DHPS (Novus), Hypusine (Millipore Sigma), EIF5A2, Cytokeratin-7 (Abcam), GAPDH (Santa Cruz; St. Louis, MO), Vimentin, E-cadherin, β-catenin, total-Smad2, or p-Smad2 (Cell Signaling).

Orthotopic ovarian cancer mouse model

To track the growth and metastasis of primary ovarian tumors in vivo, luciferase-labeled wild-type, DHPS KO, and control OVCAR8 cells were used. Based on our previous studies[18]and the method described in previous study[38], 5 mice per group is sufficient to obtain the statistical analysis for our experiment design. For investigating the impact of DHPS KO in OC cells on ovarian tumor metastasis, ten two-month-old immunocompromised NOD.Cg Prkdcscid Il2rgtm1Wjl/SzJ (NSG) female mice (#005557, Jackson Laboratory) were randomly divided into two groups. The mice were intrabursally injected with 5×10^5 DHPS KO and control OVCAR8 cells. To assess the efficacy of GC7, ten two-month-old NSG female mice were intrabursally injected with 5×10^5wild-type OVCAR8 cells. After one-week post-injection, the mice were randomly assigned to two groups. One group received GC7 treatment (8 mg/kg body weight), while the other group received vehicle treatment. The treatments were administered through intraperitoneal injection for 5 days a week over a period of 4 weeks. Since it is impossible to measure length and width to calculate the volume of tumor, the tumor progression was monitored by Xenogen Imaging system by measuring the luciferase activity. The endpoint was determined based on our previous studies[18], when the significance between groups could be determined based on the luciferase activity. After five weeks of cell injection, the mice were sacrificed by cervical dislocation after anesthesia using 5% isoflurane inhalation, both primary tumors from the ovaries and metastatic tumors from other peritoneal organs were collected. The weight of each mouse was not recorded but the condition of mouse was carefully monitored during the experiment, and they were all in good condition before being sacrificed. Double-blind histopathological analysis of the xenograft tumors and peritoneal organs was conducted by a pathologist.

Statistical analysis

All data were analyzed using GraphPad Prism 9. Significant differences between at least two independent experiments were determined by one-way ANOVA (one-way ANOVA) and student's t-test, and the data were expressed as mean ± SD. $P<0.05$ was considered as statistically significant.

Data availability

Data is provided within the manuscript or supplementary information files.

Received: 10 June 2024; Accepted: 3 January 2025
Published online: 06 January 2025

References

1. Webb, P. M. & Jordan, S. J. Epidemiology of epithelial ovarian cancer. *Best Pract. Res. Clin. Obstet. Gynaecol.* **41**, 3–14 (2017).
2. Chandra, A. et al. Ovarian cancer: current status and strategies for improving therapeutic outcomes. *Cancer Med.* **8** (16), 7018–7031 (2019).
3. Nakayama, K., Nakayama, N., Katagiri, H. & Miyazaki, K. Mechanisms of ovarian cancer metastasis: biochemical pathways. *Int. J. Mol. Sci.* **13** (9), 11705–11717 (2012).
4. Dochez, V. et al. Biomarkers and algorithms for diagnosis of ovarian cancer: CA125, HE4, RMI and ROMA, a review. *J. Ovarian Res.* **12** (1), 28 (2019).
5. Drasin, D. J., Robin, T. P. & Ford, H. L. Breast cancer epithelial-to-mesenchymal transition: examining the functional consequences of plasticity. *Breast Cancer Res.* **13** (6), 226 (2011).
6. DiMeo, T. A. et al. A novel lung metastasis signature links wnt signaling with cancer cell self-renewal and epithelial-mesenchymal transition in basal-like breast cancer. *Cancer Res.* **69** (13), 5364–5373 (2009).
7. Micalizzi, D. S., Farabaugh, S. M. & Ford, H. L. Epithelial-mesenchymal transition in cancer: parallels between normal development and tumor progression. *J. Mammary Gland Biol. Neoplasia.* **15** (2), 117–134 (2010).
8. Lili, L. N. et al. Molecular profiling supports the role of epithelial-to-mesenchymal transition (EMT) in ovarian cancer metastasis. *J. Ovarian Res.* **6** (1), 49 (2013).
9. Ahmed, N., Abubaker, K., Findlay, J. & Quinn, M. Epithelial mesenchymal transition and cancer stem cell-like phenotypes facilitate chemoresistance in recurrent ovarian cancer. *Curr. Cancer Drug Targets.* **10** (3), 268–278 (2010).
10. Yan, H. & Sun, Y. Evaluation of the mechanism of epithelial-mesenchymal transition in human ovarian cancer stem cells transfected with a WW domain-containing oxidoreductase gene. *Oncol. Lett.* **8** (1), 426–430 (2014).
11. Park, M. H., Nishimura, K., Zanelli, C. F. & Valentini, S. R. Functional significance of eIF5A and its hypusine modification in eukaryotes. *Amino Acids.* **38** (2), 491–500 (2010).
12. Clement, P. M. et al. Identification and characterization of eukaryotic initiation factor 5A-2. *Eur. J. Biochem.* **270** (21), 4254–4263 (2003).
13. Jenkins, Z. A., Haag, P. G. & Johansson, H. E. Human eIF5A2 on chromosome 3q25-q27 is a phylogenetically conserved vertebrate variant of eukaryotic translation initiation factor 5A with tissue-specific expression. *Genomics* **71** (1), 101–109 (2001).
14. Clement, P. M., Johansson, H. E., Wolff, E. C. & Park, M. H. Differential expression of eIF5A-1 and eIF5A-2 in human cancer cells. *FEBS J.* **273** (6), 1102–1114 (2006).
15. Yang, G. F. et al. Expression and amplification of eIF-5A2 in human epithelial ovarian tumors and overexpression of EIF-5A2 is a new independent predictor of outcome in patients with ovarian carcinoma. *Gynecol. Oncol.* **112** (2), 314–318 (2009).
16. Wu, G. Q., Xu, Y. M. & Lau, A. T. Y. Recent insights into eukaryotic translation initiation factors 5A1 and 5A2 and their roles in human health and disease. *Cancer Cell. Int.* **20**, 142 (2020).
17. Guan, X. Y. et al. Isolation of a novel candidate oncogene within a frequently amplified region at 3q26 in ovarian cancer. *Cancer Res.* **61** (9), 3806–3809 (2001).
18. Zhao, G. et al. EIF5A2 controls ovarian tumor growth and metastasis by promoting epithelial to mesenchymal transition via the TGFbeta pathway. *Cell. Biosci.* **11** (1), 70 (2021).
19. Mathews, M. B. & Hershey, J. W. The translation factor eIF5A and human cancer. *Biochim. Biophys. Acta.* **1849** (7), 836–844 (2015).
20. Wang, F. W., Guan, X. Y. & Xie, D. Roles of eukaryotic initiation factor 5A2 in human cancer. *Int. J. Biol. Sci.* **9** (10), 1013–1020 (2013).

21. Guth, R. et al. DHPS-dependent hypusination of eIF5A1/2 is necessary for TGFbeta/fibronectin-induced breast cancer metastasis and associates with prognostically unfavorable genomic alterations in TP53. *Biochem. Biophys. Res. Commun.* **519** (4), 838–845 (2019).
22. Bandino, A., Geerts, D., Koster, J. & Bachmann, A. S. Deoxyhypusine synthase (DHPS) inhibitor GC7 induces p21/Rb-mediated inhibition of tumor cell growth and DHPS expression correlates with poor prognosis in neuroblastoma patients. *Cell. Oncol. (Dordr)*. **37** (6), 387–398 (2014).
23. Jakus, J., Wolff, E. C., Park, M. H. & Folk, J. E. Features of the spermidine-binding site of deoxyhypusine synthase as derived from inhibition studies. Effective inhibition by bis- and mono-guanylated diamines and polyamines. *J. Biol. Chem.* **268** (18), 13151–13159 (1993).
24. Fang, L., Gao, L., Xie, L. & Xiao, G. GC7 enhances cisplatin sensitivity via STAT3 signaling pathway inhibition and eIF5A2 inactivation in mesenchymal phenotype oral cancer cells. *Oncol. Rep.* **39** (3), 1283–1291 (2018).
25. Lou, B. et al. N1-guanyl-1,7-diaminoheptane (GC7) enhances the therapeutic efficacy of doxorubicin by inhibiting activation of eukaryotic translation initiation factor 5A2 (eIF5A2) and preventing the epithelial-mesenchymal transition in hepatocellular carcinoma cells. *Exp. Cell. Res.* **319** (17), 2708–2717 (2013).
26. Liu, Y. et al. N1-Guanyl-1,7-Diaminoheptane sensitizes estrogen receptor negative breast Cancer cells to Doxorubicin by preventing epithelial-mesenchymal transition through inhibition of eukaryotic translation initiation factor 5A2 activation. *Cell. Physiol. Biochem.* **36** (6), 2494–2503 (2015).
27. Park, S. J., Yoon, B. H., Kim, S. K. & Kim, S. Y. GENT2: an updated gene expression database for normal and tumor tissues. *BMC Med. Genomics*. **12** (Suppl 5), 101 (2019).
28. Gyorffy, B. Discovery and ranking of the most robust prognostic biomarkers in serous ovarian cancer. *Geroscience* (2023).
29. Wang, C. et al. Extracellular signal-regulated kinases associate with and phosphorylate DHPS to promote cell proliferation. *Oncogenesis* **9** (9), 85 (2020).
30. Schultz, C. R. et al. Synergistic drug combination GC7/DFMO suppresses hypusine/spermidine-dependent eIF5A activation and induces apoptotic cell death in neuroblastoma. *Biochem. J.* **475** (2), 531–545 (2018).
31. Tang, D. J. et al. Overexpression of eukaryotic initiation factor 5A2 enhances cell motility and promotes tumor metastasis in hepatocellular carcinoma. *Hepatology* **51** (4), 1255–1263 (2010).
32. Chakraborty, S. et al. De novo and histologically transformed small cell lung cancer is sensitive to lurbinectedin treatment through the modulation of EMT and NOTCH signaling pathways. *Clin. Cancer Res.* **29** (17), 3526–3540 (2023).
33. Hu, C. et al. Methylmalonic acid promotes colorectal cancer progression via activation of Wnt/beta-catenin pathway mediated epithelial-mesenchymal transition. *Cancer Cell. Int.* **23** (1), 131 (2023).
34. Chen, Z. et al. SHH/GLI2-TGF-beta1 feedback loop between cancer cells and tumor-associated macrophages maintains epithelial-mesenchymal transition and endoplasmic reticulum homeostasis in cholangiocarcinoma. *Pharmacol. Res.* **187**, 106564 (2023).
35. Citarella, A. et al. Hedgehog-GLI and notch pathways sustain Chemoresistance and Invasiveness in Colorectal Cancer and their inhibition restores Chemotherapy Efficacy. *Cancers (Basel)* **15**(5) (2023).
36. Zhang, J. et al. Isotoosendanin exerts inhibition on triple-negative breast cancer through abrogating TGF-beta-induced epithelial-mesenchymal transition via directly targeting TGFbetaR1. *Acta Pharm. Sin B.* **13** (7), 2990–3007 (2023).
37. Chen, Z. et al. Doxycycline inducible kruppel-like factor 4 lentiviral vector mediates mesenchymal to epithelial transition in ovarian cancer cells. *PLoS One*. **9** (8), e105331 (2014).
38. Arifin, W. N. & Zahiruddin, W. M. Sample size calculation in Animal studies using resource equation Approach. *Malays J. Med. Sci.* **24** (5), 101–105 (2017).

Acknowledgements

This study was partially supported by a grant R21CA216585-01A1 (JY) from the NCI; a UTHSC CORNET award (JY, WZ). The content is solely the responsibility of the authors and does not necessarily represent the official views of the NIH.

Author contributions

Conceptualization & designs JY and WZ.; Data Collection and Analysis, GZ, XZ, ZL, WZ, and JY; Review and Writing, JY, WZ, XZ, ZL, BW, PD, HW, LMP, and GT. All authors have read and agreed to the published version of the manuscript.

Declarations

Ethics approval and consent to participate

All animal experiments were conducted according to the Institutional Animal Care and Use Committee (IACUC) approval at the University of Tennessee Health Science Center. Paraffin-embedded ovarian sections of HGSC were obtained from de-identified ovarian patient biopsy specimens (UTHSC Tissue Services Core).

Competing interests

The authors declare no competing interests.

Additional information

Supplementary Information The online version contains supplementary material available at https://doi.org/10.1038/s41598-025-85466-5.

Correspondence and requests for materials should be addressed to W.Z. or J.Y.